Placenta 171 (2025) 178–187

Contents lists available at ScienceDirect

Placenta

journal homepage: www.elsevier.com/locate/placenta

Endothelial responses to angiogenic modulators highlight metabolic mechanisms underlying vascular dysfunction in preeclampsia

Priscila R. Nunes [a], Ricardo M. Bruder [a], Julyane N.S. Kaihara [a], Fabio R. de Moraes [b], Ljubica Tasic [c], Raquel L. Bernardino [d,e], Patricia Braga [d,e], Pedro F. Oliveira [f], Irene Rebelo [g,h], Margarida Fardilha [i], Ricardo C. Cavalli [j], Valeria C. Sandrim [a,*], Marco G. Alves [i,**]

[a] Department of Biophysics and Pharmacology, Institute of Biosciences, Sao Paulo State University (Unesp), Botucatu, SP, Brazil
[b] Multiuser Center for Biomolecular Innovation, Department of Physics, Institute of Biosciences, Languages and Exact Sciences, Sao Paulo State University (Unesp), Sao Jose Do Rio Preto, SP, Brazil
[c] Department of Organic Chemistry, Institute of Chemistry, Universidade Estadual de Campinas (Unicamp), Campinas, SP, Brazil
[d] Unit for Multidisciplinary Research in Biomedicine (UMIB), Institute of Biomedical Sciences Abel Salazar (ICBAS), University of Porto, Porto, Portugal
[e] ITR- Laboratory for Integrative and Translational Research in Population Health, Porto, Portugal
[f] LAQV-REQUIMTE and Department of Chemistry, University of Aveiro, Aveiro, Portugal
[g] UCIBIO-REQUIMTE, Laboratory of Biochemistry, Department of Biologic Sciences, Pharmaceutical Faculty, University of Porto, 4050-313, Porto, Portugal
[h] Associate Laboratory i4HB- Institute for Health and Bioeconomy, Laboratory of Biochemistry, Department of Biologic Sciences, Pharmaceutical Faculty, University of Porto, 4050-313, Porto, Portugal
[i] iBiMED - Institute of Biomedicine and Department of Medical Sciences University of Aveiro, Aveiro, Portugal
[j] Department of Gynecology and Obstetrics, Faculty of Medicine of Ribeirao Preto, University of Sao Paulo (USP), Ribeirao Preto, SP, Brazil

ARTICLE INFO

Keywords:
Preeclampsia
sFlt-1/PlGF ratio
Angiogenic imbalance
Metabolism
Metabolites
Mitochondrial dysfunction

ABSTRACT

Introduction: An elevated sFlt-1/PlGF ratio in preeclampsia (PE) directly impairs endothelial cell (EC) metabolism, leading to increased lactate dehydrogenase (LDH) release, lipid peroxidation, and mitochondrial dysfunction. This may reflect a distinct metabolite profile which correlates with systemic maternal metabolic dysregulation, as evidenced by the association between circulating sFlt-1 and succinate/glycine levels.
Methods: A cross-sectional case-control study was performed on plasma of PE patients (n = 54) in addition to an *in vitro* study using ECs. We correlated plasma metabolite profiles (by nuclear magnetic resonance-based metabolomics) with sFlt-1 levels (by Enzyme-Linked Immunosorbent Assay). Mechanistically, we examined the impact of varying sFlt-1/PlGF ratios on EC function and metabolism after 24 h, assessing cell viability, cytotoxicity, proliferation, oxidative stress-related damage (lipid peroxidation and nitration), and real-time mitochondria function and metabolic profiles.
Results: In pregnant women with PE, circulating sFlt-1 levels positively correlated with succinate and glycine levels, but not significantly with lactate or glucose. *In vitro*, as sFlt-1/PlGF ratios, increased EC damage (LDH release) and oxidative stress-related damage (4-hydroxy-2-nonenal) increased dose-dependently. High sFlt-1/PlGF ratios also increased mitochondrial spare respiratory capacity, suggesting a compensatory mechanism. Metabolomics revealed metabolic reprogramming in ECs exposed to varying sFlt-1/PlGF ratios, with significant alterations in lactate, succinate, glucose, and glycine levels.
Discussion: These correlations and *in vitro* changes suggest a mechanistic link between sFlt-1/PlGF ratios, oxidative stress-related damage, and metabolic reprogramming in ECs, which could be targeted for therapeutics. Furthermore, the identification of succinate and glycine as key metabolites associated with sFlt-1 levels and sFlt-1/PlGF ratios may provide novel biomarkers for disease risk stratification and/or monitoring PE progression.

* Corresponding author.
** Corresponding author.
E-mail addresses: valeria.sandrim@unesp.br (V.C. Sandrim), marcoalves@ua.pt (M.G. Alves).

https://doi.org/10.1016/j.placenta.2025.09.018
Received 3 April 2025; Received in revised form 22 September 2025; Accepted 23 September 2025
Available online 25 September 2025

1. Introduction

Preeclampsia (PE) is a hypertensive disorder of pregnancy, characterized by multiorgan system damage in the liver, kidney, and brain, often accompanied by proteinuria, coagulation complications, pulmonary edema, and/or neurological manifestations. This condition arises from abnormal placentation, which can lead to fetal growth restriction, low birth weight, and/or preterm birth. Globally, PE increases perinatal and maternal morbidity and mortality, affecting 2–8 % of pregnancies [1].

The pathogenesis of PE remains incompletely understood, but a crucial imbalance between pro- and anti-angiogenic factors has been identified [2]. This imbalance is characterized by an excess of anti-angiogenic factors, such as soluble fms-like tyrosine kinase 1 (sFlt-1), relative to pro-angiogenic factors, such as vascular endothelial growth factor (VEGF) and placental growth factor (PlGF) [3–5]. sFlt-1 binds to VEGF and PlGF, effectively reducing their availability. An increase in circulating sFlt-1 is thought to occur due to placental hypoxia, which in turn decreases the concentrations of free VEGF and PlGF [6].

PE is associated with increased levels of circulating sFlt-1, which is primarily responsible for endothelial dysfunction, and decreased PlGF levels. This imbalance not only precedes the clinical onset of the disease, but also persists throughout its course [7]. sFlt-1 levels typically increase approximately 4–6 weeks before PE manifestation, while PlGF levels decrease simultaneously [8,9]. Consequently, the sFlt-1/PlGF ratio is believed to be a more reliable tool for PE prediction than the individual measurements of these markers [7,10–12]. An imbalance of angiogenic factors (increased sFlt-1 and decreased PlGF) is strongly implicated in PE development [3–5]. The sFlt-1/PlGF ratio has shown efficacy in early detection and complication prevention, but it has yet to be adopted as a diagnostic standard for PE. Thus, investigating this ratio's impact on endothelial cell (EC) metabolism and oxidative stress is crucial for understanding PE pathogenesis and improving its diagnosis and management. A prospective, international, observational study (PROGNOSIS study) evaluated the use of an sFlt-1/PlGF ratio cut-off threshold to rule out (within one week) or rule in (within four weeks) PE, eclampsia, or HELLP syndrome [10]. This study demonstrated that an sFlt-1/PlGF ratio equal to or below 38 has a 99.3 % probability of no PE development. Furthermore, a retrospective study with 1117 patients revealed that women who presented with signs and symptoms of PE had a significantly higher median sFlt-1/PlGF ratio (177; interquartile range, 54–362) compared with those without these outcomes (14; interquartile range 4–64) [13]. An elevated sFlt-1/PlGF ratio is implicated in the pathological changes observed in PE, such as oxidative [14,15] and endoplasmic reticulum stress [16], as well as alterations in maternal endothelial responses [17]. Shinohara et al. also showed a correlation between the sFlt-1/PlGF ratio and severe negative consequences in PE, suggesting its use in assessing risk and managing women diagnosed with early-onset PE [18]. Furthermore, *in vitro* studies using umbilical arteries have shown that the sFlt-1/PlGF ratio directly influences vascular tone during pregnancy [19].

Mitochondrial dysfunction, characterized by reduced ATP production and increased reactive oxygen species (ROS) generation, is increasingly recognized as a key factor in PE development. Placental-derived factors, including inflammatory cytokines, anti-angiogenic factors, extracellular vesicles, debris, and cell-free fetal DNA, contribute to mitochondrial anomalies and endothelial dysfunction [20–22]. In PE, a vicious cycle of mitochondrial dysfunction and oxidative stress perpetuates endothelial damage [23,24]. This is critical in the placenta, a metabolically active organ highly dependent on glucose (responsible for 30 % of maternal blood glucose uptake), where ATP production is dynamically regulated and influenced by several factors. The rate of glucose uptake in the placenta depends on ATP production via oxidative phosphorylation, which is influenced by placental structure, permeability, fetal growth, and placental weight [25].

Therefore, to investigate the clinical impact of the angiogenic imbalance in PE, we correlated maternal plasma metabolic profiles with sFlt-1 levels, aiming to identify a systemic metabolic signature of the disease. In parallel, we explored the mechanistic underpinnings of this association by examining the impact of varying sFlt-1/PlGF ratios (low, medium, and high) on EC function and metabolism.

2. Materials and methods

2.1. Study population

This cross-sectional case-control study was approved by the Institutional Review Board from the Ribeirao Preto Medical School of the University of Sao Paulo, Brazil (FMRP/USP, protocol code 37738620.0.0000.5440, on October 19, 2020). The procedures were conducted in compliance with both the Declaration of Helsinki and the applicable institutional policies and regulations for studies involving human subjects. At clinical attendance, participants were recruited voluntarily, and all provided written informed consent. If there were pregnant women under the age of 18, their parents or legal guardians were required to give written consent. For research purposes, we accessed the clinical data of the samples archived on July 13, 2023. We enrolled a total of 54 preeclamptic pregnant women from the Department of Obstetrics and Gynecology, University Hospital of the Ribeirao Preto Medical School (HCFMRP). The diagnostic criteria of PE included hypertension (systolic blood pressure $\geq$140 mmHg and/or diastolic blood pressure $\geq$90 mmHg) in women previously normotensive after 20 weeks of gestation accompanied by proteinuria. In the absence of proteinuria, hypertension with symptoms of damage to the end-organs was considered. [1]. Pregnancies with fetal or hemostatic abnormalities, chronic hypertension, cancer, diabetes mellitus, cardiovascular conditions, or autoimmune, renal, or hepatic diseases were excluded.

2.2. Plasma collection and determination of circulating sFlt-1 levels

Upon PE diagnosis, venous blood was collected into sterile tubes with 10 U/mL EDTA (Becton Dickinson-BD Vacutainer; BD Biosciences, Franklin Lakes, NJ, USA). Tubes were centrifuged at 1500 g for plasma separation, and aliquots were stored at − 80 °C. Circulating sFlt-1 levels were quantified in duplicate using a commercially available Enzyme-Linked Immunosorbent Assay (ELISA) kit (Catalog number: DVR100B, R&D Systems, Minneapolis, MN, USA) following manufacturer's instructions.

2.3. Cell culture and incubation with varying sFlt-1/PlGF ratios

Human umbilical vein endothelial cells (HUVEC) (Ea.hy926 – CLS, Eppelheim, Germany) were cultured in Dulbecco's Modified Eagle Medium (DMEM/F12, Gibco, Massachusetts, USA) at 5 % CO_2 supplemented with 10 % (v/v) fetal bovine serum (FBS), 100 IU/mL penicillin, 100 μg/mL streptomycin and 2 mmol/L L-glutamine (Sigma-Aldrich, San Luis, USA). At 80 % confluence cells were incubated for 24 h in medium containing sFlt-1/PlGF (R&D Systems/Bio-Techne, Milan, Italy, catalog numbers: 3516-FL-050 and 264-PGB-010) at following concentrations: 1.6 (sFlt-1: 10 ng/mL and PlGF: 6 ng/mL), 33.3 (sFlt-1: 1000 ng/mL and PlGF: 30 ng/mL) or 85.7 (sFlt-1: 1800 ng/mL and PlGF: 21 ng/mL). These concentrations were based on the use of the sFlt1/PlGF ratios for short-term prediction and confirmation of PE [26]. All treatment groups were compared with untreated ECs cultured under identical conditions, which served as the baseline control. All experiments were performed in three biological replicates and five technical replicates, except for the real-time mitochondrial function analyses and NMR-based metabolomics (Figs. 3 and 4, where four biological replicates and five biological replicates were conducted, respectively). For statistical analysis, the average of the technical replicates was calculated and used as the representative value of each biological replicate.

2.4. Assessments of cell viability and proliferation

The viability of the ECs was assessed by using the MTT (3-(4,5-dimethylthiazol-2-yl)-2,5-diphenyltetrazolium bromide) reduction assay (Merck) as described previously [27]. Absorbance was measured at 570 and 655 nm on a BioTek Synergy HT microplate multi-reader (BioTek, Vermont, USA). The proliferation of ECs was assessed using the Sulforhodamine B (SRB) colorimetric assay (Thermo Fisher - Massachusetts, USA). In brief, $5x10^4$ cells were cultured per well in a 24-well plate until reaching 60–70 % confluence. After 24 h of incubation with the different treatments, the cells were fixed with a 1 % acetic acid solution in 99 % methanol for at least 1 h at −20 °C. Then, the cells were incubated with a 0.05 % SRB solution prepared with 1 % acetic acid in water for 1 h at 37 °C. After washing the cells with 1 % acetic acid solution and solubilized with 10 mmol/L Tris solution (pH 10). Then, 100 μL of supernatant was transferred to a 96-well plate and absorbance was determined at 490 nm using a BioTek Synergy HT microplate reader (BioTek).

2.5. Lactate dehydrogenase (LDH) cytotoxicity assay

Extracellular LDH activity was determined by using commercial LDH-CytoxTM Assay Kit (Thermo Fisher), following the manufacturer's instructions. In brief, after 24 h treatment, 100 μL of supernatant was transferred to a 96-well plate and then 100 μL LDH assay substrate was added to all samples and left in the dark at 37 °C for 30 min. The absorbance of all samples was then measured at 490 nm using the BioTek Synergy HT microplate reader (BioTek).

2.6. Protein extraction

For protein extraction, 1.50 – $5x10^5$ cells were seeded in 6-well plates and treated with sFlt-1/PlGF ratios for 24 h. Following treatment, cells were detached and collected by centrifugation (500×*g*; 10 min). Total protein was then extracted from the pelleted cells using radioimmunoprecipitation assay (RIPA) supplemented with a 1 % protease inhibitor cocktail and 10 mmol/L sodium orthovanadate. In brief, 50 μL of supplemented RIPA buffer were added to the pelleted cells and the resuspended samples were subjected to gentle shaking at 4 °C for 20 min. A Pierce™ Microplate BCA Protein Assay kit (Thermo Fisher) was used for protein quantification in the protein extracts according to the manufacturer's instructions. Different concentrations of bovine serum albumin (BSA, Thermo Fisher) were used as standards for calibration. Absorbance was measured at 560 nm using the BioTek Synergy HT microplate multi-reader (BioTek).

2.7. Analyses of protein nitration and lipid peroxidation

To measure protein nitration and lipid peroxidation, the slot-blot technique was used. Protein extracts from each sample were diluted to a concentration of 0.05 μg/μL using PBS and transferred to a polyvinylidene difluoride – PVDF membrane (Merck). The membrane was previously activated for 1 min in methanol, 5 min in distilled H_2O, and 15 min in PBS. The technique was performed using a Hybrid-Slot manifold system (Biometra, Göttingen, Germany). The membrane was then blocked for 60 min with 5 % non-fat milk and incubated overnight with rabbit anti-3-nitrotyrosine (1:1000 – Cell Signaling, Massachusetts, USA) and goat anti-4-hydroxynonenal (1:2500 – Abcam, Cambridge, UK). The immunoreactive proteins were detected with a goat anti-rabbit IgG-HRP secondary antibody (1:5000 - Abcam). The membrane was then reacted with WesternBright™ ECL (Advansta, Menlo Park, CA, USA) and visualized on the Chemidoc MP Imaging System (Bio-Rad, California, USA). The densities of each band were obtained with Image Lab Software 5.1 (Bio-Rad).

2.8. Real-time analysis of mitochondrial function

To assess mitochondrial function in real-time, 7.5 x 10^4 cells were seeded in Seahorse XF24 cell culture microplates (Agilent Technologies, Texas, USA) with standard growth medium; at 70–80 % confluence. The cells were then incubated for 24 h with the different treatment conditions. After the incubation period, the culture medium was exchanged for the assay medium (XF DMEM base medium supplemented with 2 mmol/L glutamine, 1 mmol/L pyruvate, and 10 mmol/L glucose) for 40 min at 37 °C in a non-CO_2 incubator. The oxygen consumption rate (OCR) was then measured using a Seahorse XF Analyzer, following the mitochondrial stress test protocol. The assay included a basal measurement phase, followed by sequential injections of oligomycin (1.5 μmol/L), FCCP (1 μmol/L), and a combination of rotenone and antimycin A (0.5 μmol/L each). Three OCR readings were recorded after each injection, with 8-min intervals between measurements, totaling 100–120 min per assay. Although extracellular acidification rate (ECAR) data were collected in parallel, they were not included in the present analysis. The data from the experiments were normalized to protein concentration, after cell lysis using the RIPA buffer and protein quantification with BCA protein assay (Thermo Fisher). Each condition was analyzed in duplicate, and all calculations were done using the Seahorse Analytics software (Agilent Technologies). The results were normalized with the mean of the control (fold variation to control).

2.9. NMR-based metabolomics

All plasma samples were thawed at 4 °C. Next, 200 μL of deuterated water (D_2O) was added to each 300 μL of individual plasma samples. Subsequently, the resulting solution was transferred to a 5 mm nuclear magnetic resonance tube, and the samples were analyzed on a Bruker Ascend™ 600 MHz spectrometer (Bruker Corporation, Billerica, MA, USA) equipped with a room-temperature TXI-Z triple inverse probe. One-dimensional ^{1}H NMR spectra were acquired using a NOESY presaturation pulse sequence (noesygppr1d), which provides excellent water suppression and is optimal for quantitative metabolomics studies. The parameters included a recycle delay of 4 s, mixing time of 150 milliseconds, 128 scans, and the collection of 64 k complex data points within a spectral width of 20 ppm. Post-acquisition, the free induction decay (FID) measurement was multiplied by an exponential function with 1 Hz line-broadening, followed by Fourier transform. The CPMG (Carr-Purcell-Meiboom Gill) pulse sequence was also employed with a 200 loop for T2 filter, effectively suppressing macromolecule signals. This sequence shared similar parameters with the noesy1d experiment, encompassing a recycle delay of 4 s, 128 scans, and 64 k complex data points.

Culture media samples were prepared by mixing 480 μL of post-treatment culture medium and 120 μL of a 10 mmol/L sodium fumarate in 0.2 mol/L phosphate buffer deuterated water solution, pH 7.0 (Sigma-Aldrich, St. Louis, MO, USA). 1D-^{1}H NMR spectra were acquired on a 500 MHz Bruker Avance III HD spectrometer equipped with a 5 mm TXI probe (Bruker Corporation, Billerica, MA, USA) 298 K. Spectra were acquired using a water-suppressed zgpr pulse sequence, sweep width of 14 ppm, 7 s relaxation delay, 2.3 s acquisition time, 30° pulse angle and 128 scans. Bruker Topsin 3.5 (Bruker Corporation) was used for the acquisition and processing of the NMR spectra. A line broadening of 0.2 Hz was applied to the FID before the Fourier transform. Spectra were manually phased, baseline corrected, and chemical shifts were internally referenced to the fumarate signal at 6.50 ppm. Sodium fumarate was used as an internal standard for metabolite quantification. For metabolite identification, two-dimensional ^{1}H–^{1}H TOCSY (Total Correlation Spectroscopy) and ^{1}H-^{13}C HSQC (Heteronuclear Single Quantum Coherence) spectra were acquired from randomly selected samples. The data processing involved the use of TopSpin software version 3.2 (Bruker Corporation), including Fourier transforms on FID signals, as well as phase and baseline corrections. Further refinement, including

reference and manual inspection of the spectra, was carried out in MestReNova 14.2.2 (2021 Mestrelab Research S.L.). Metabolite identification spanned amino acids, ketone bodies, fatty acids, and polar molecules facilitated by Chenomx NMR Suite software version 9.02 (Chenomx Inc., Edmonton, AB, Canada). This involved comparing peak spectra, chemical shifts (in ppm), and scalar couplings (J) with the Spectral Reference Library of the software, aligning with the conditions under which the data was acquired, including pH, temperature, and NMR field strength. When signals were not cataloged in the Chenomx software database, the Human Metabolome Database (HMDB) [28] was referenced.

2.10. Integrated statistical and data analyses

Statistical analyses were performed using the parametric one-way ANOVA test followed by Bonferroni's test after performing the normality test. Values of clinical characteristics are given as mean ± standard deviation for parametric variables; median [minimum – maximum] for non-parametric variables; and absolute numbers (frequency in percentage) for categorical variables. Pearson correlation test was employed to evaluate the relationship between plasma sFlt-1 levels and ten circulating metabolites (acetate, alanine, glucose, glutamine, glycine, isoleucine, lactate, succinate, tyrosine, valine). Results with a p-value <0.05 were considered significant. GraphPad Prism version 9.5 (GraphPad Software Inc., San Diego, CA, USA) was used to perform these analyses. Metabolomics data were Pareto scaled before further analysis. Chemometric analyses comprising principal component analysis (PCA) and partial least squares discriminant analysis (PLS-DA) were employed. A variable importance in projection (VIP) score was generated, visually representing the significance of specific metabolites in distinguishing the experimental groups. A threshold higher than 1.0 was considered relevant. To compare differences in cell media metabolite concentrations between experimental groups, we conducted univariate analyses using one-way ANOVA followed by Fisher's post-hoc tests, with a p-value <0.05. All chemometric and univariate analyses were conducted using the online software MetaboAnalyst, versions 5.0 and 6.0 (http://www.metaboanalyst.ca/).

3. Results

3.1. Clinical features of PE in pregnant women

Table 1 shows the clinical characteristics of the PE patients included in the study. Thirty-two percent (n = 16) were primiparous. While all participants met the diagnostic criteria for PE, some had blood pressure readings below 140/90 mmHg due to the use of antihypertensive medications, including methyldopa, nifedipine, and/or hydralazine. The median systolic blood pressure (SBP) was 140 mmHg, ranging from 110 to 200 mmHg. The median diastolic blood pressure (DBP) was 80 mmHg, ranging from 60 to 130 mmHg. The median 24 h-proteinuria was 431 mg, with a wide range from 302 to 5945 mg, reflecting the varying severity of proteinuria in PE. The median plasma sFlt-1 level was 9.9 pg/mL, ranging from 0.3 to 20.6 pg/mL. The median gestational age at delivery was 37 weeks, ranging from 22 to 41 weeks, indicating a mix of preterm and term deliveries. Twenty-eight-point three percent (n = 13) of newborns had an Apgar score at 1 min of less than 7, while 4.4 % (n = 2) had an Apgar score at 5 min of less than 7. This data reflects potential complications associated with PE and premature birth.

Table 1
Clinical and demographic characteristics of the PE cohort (n = 54).

Parameter	PE cohort (n = 54)
Age (years)	28.8 ± 7.1
Primiparity (%)	16 (32)
BMI (kg/m^2)	33.7 ± 6.7
SBP (mmHg)	140 [110–200]
DBP (mmHg)	80 [60–130]
HR (bpm)	80 [60–96]
AST (U/L)	16 [5–54]
Creatinine (mg/dL)	0.7 [0.4–2.9]
24 h Pr (mg/24 h)	431 [302–5945]
Plasma sFlt-1 (ng/mL)	9.9 [0.3–32]
GAD (weeks)	37 [22–41]
Newborn Weight (g)	2915 [400–4235]
APGAR Score 1 (1 min) < 7 (%)	13 (28.3)
APGAR Score 2 (5 min) < 7 (%)	2 (4.4)

Abbreviations: 24 h Pr, 24 h proteinuria; AST, aspartate transaminase; BMI, body mass index; DBP, diastolic blood pressure; GAD, gestational age at delivery; HR, heart rate; SBP, systolic blood pressure. Values are given as mean ± standard deviation for parametric variables; median [minimum – maximum] for non-parametric variables; and absolute numbers (frequency in percentage) for categorical variables.

3.2. Plasma succinate and glycine levels positively correlated with sFlt-1 levels in PE pregnant women

Correlation analyses were performed between circulating levels of the sFlt-1 and plasma levels of ten quantified metabolites in women with PE. Of these, four metabolites—lactate, succinate, glucose, and glycine—are presented here, as they were also found to be altered in conditioned media from the ECs cultured with varying sFlt-1/PlGF ratios. Lactate levels in women with PE tended to increase with higher sFlt-1 levels, although this positive correlation did not reach statistical significance ($r = 0.26$, $p = 0.07$) (Fig. 1A). A positive correlation was observed between succinate and sFlt-1 levels ($r = 0.40$, $p = 0.004$) (Fig. 1B). Conversely, no correlation was found between glucose and sFlt-1 levels ($r = -0.09$, $p = 0.52$) (Fig. 1C). Glycine levels also demonstrated a statistically significant positive correlation with sFlt-1 ($r = 0.33$, $p = 0.02$) (Fig. 1D). All data represent individual patient values with lines of best fit and 95 % confidence intervals (CIs) shown. Correlation results for the remaining six quantified metabolites, all of which were not correlated with sFlt-1 ($p > 0.05$), are provided in Supplementary Table S1.

3.3. Increased sFlt-1/PlGF ratios induce EC damage and oxidative stress

To explore the mechanistic underpinnings of the association between sFlt-1 levels and plasma metabolite concentrations in women with PE, we examined the impact of varying sFlt-1/PlGF ratios (low, medium, and high) on EC function and metabolism. While data points are scattered across the different ratios, neither cell viability nor proliferation appear to be substantially affected by changes in sFlt-1/PlGF ratio, as the mean values for all conditions remain close to 1.0. However, we detected a clear dose-dependent increase in LDH release with increasing the sFlt-1/PlGF ratios (Fig. 2A). As the sFlt-1/PlGF ratio increases, there was a significant elevation in LDH release at the highest ratio, indicative of increased cellular damage. To investigate the effects of varying sFlt-1/PlGF ratios on EC oxidative stress, we measured the levels of 4-hydroxynonenal (4-HNE), a marker of lipid peroxidation (Fig. 2B), and 3-nitrotyrosine, a marker of protein nitration (Fig. 2C). Fig. 2 shows the levels of 4-HNE (Panel B) and 3-nitrotyrosine (Panel C) in ECs after exposure to low, medium, and high sFlt-1/PlGF ratios. 4-HNE levels were significantly elevated in ECs exposed to the high sFlt-1/PlGF ratio compared with those exposed to the low ratio ($p < 0.05$) (Fig. 2B). While a similar trend was observed for 3-nitrotyrosine, with the ECs subjected to the high sFlt-1/PlGF ratio exhibiting the highest levels, but this increase was not statistically significant ($p = 0.36$).

3.4. A high sFlt-1/PlGF ratio increases real-time spare respiratory capacity in ECs

Analysis of mitochondrial function revealed no significant alterations in response to varying sFlt-1/PlGF ratios. We observed no

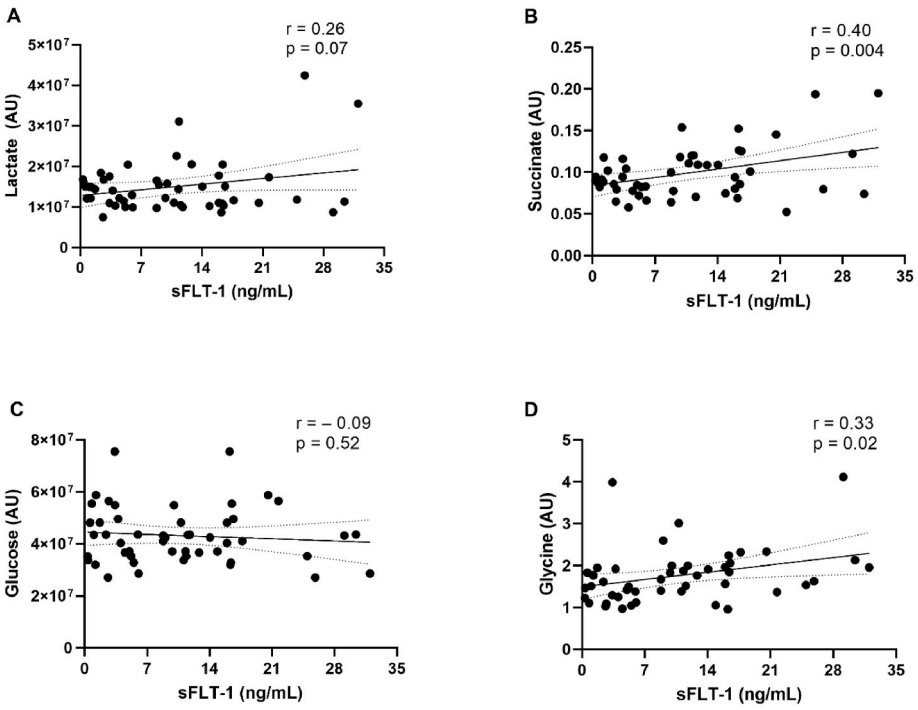

Fig. 1. Correlation between circulating sFlt-1 levels and plasma metabolite concentrations in women with PE. (A) Lactate, (B) Succinate, (C) Glucose, and (D) Glycine. Pearson's correlation coefficients (r) and associated P-values are shown for each correlation. AU denotes arbitrary units.

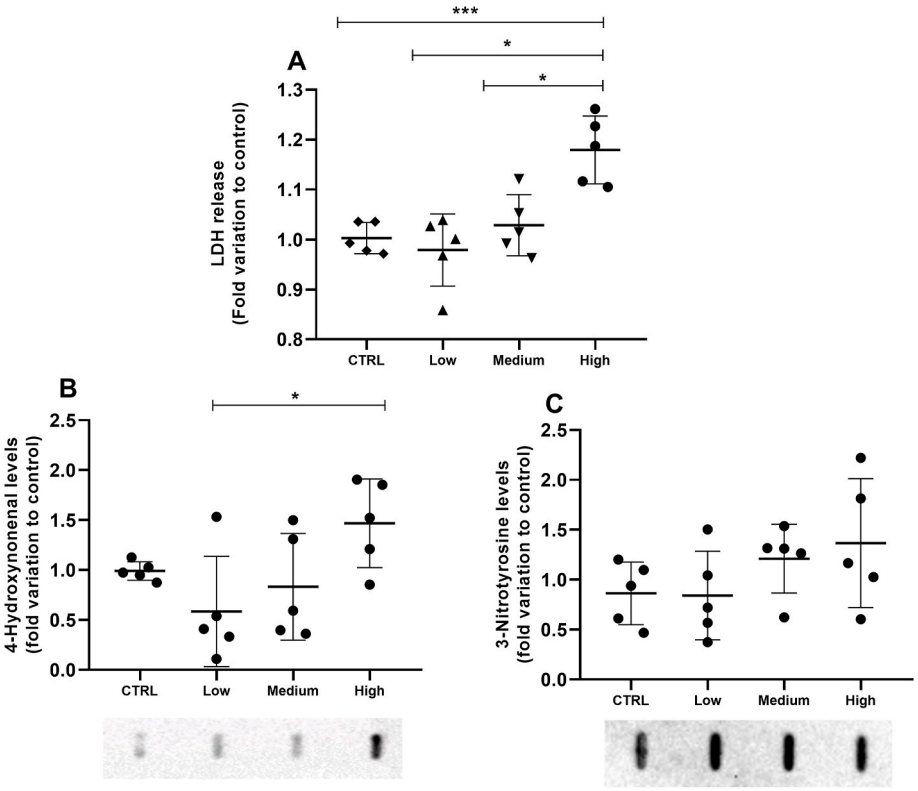

Fig. 2. Effects of sFlt-1/PlGF ratios on EC damage and oxidative stress. ECs were untreated or treated for 24 h with low, medium, or high sFlt-1/PlGF ratios (1.6, 33.3, and 85.7, respectively). (A) LDH release, (B) 4-HNE levels, and (C) 3-nitrotyrosine levels are shown as fold variation relative to CTRL. Data are presented as mean ± SD (n = 5 per group). Statistical significance was determined by one-way ANOVA followed by Bonferroni's post-hoc test. *$p < 0.05$; ***$p < 0.001$.

significant differences among the groups in: basal respiration, which reflects the cell's steady-state energy demand (Fig. 3A); maximal respiration, which indicates the total respiratory capacity (Fig. 3B); or non-mitochondrial oxygen consumption (Fig. 3C). ATP-production coupled respiration, representing the portion of cellular respiration specifically dedicated to ATP generation via oxidative phosphorylation,

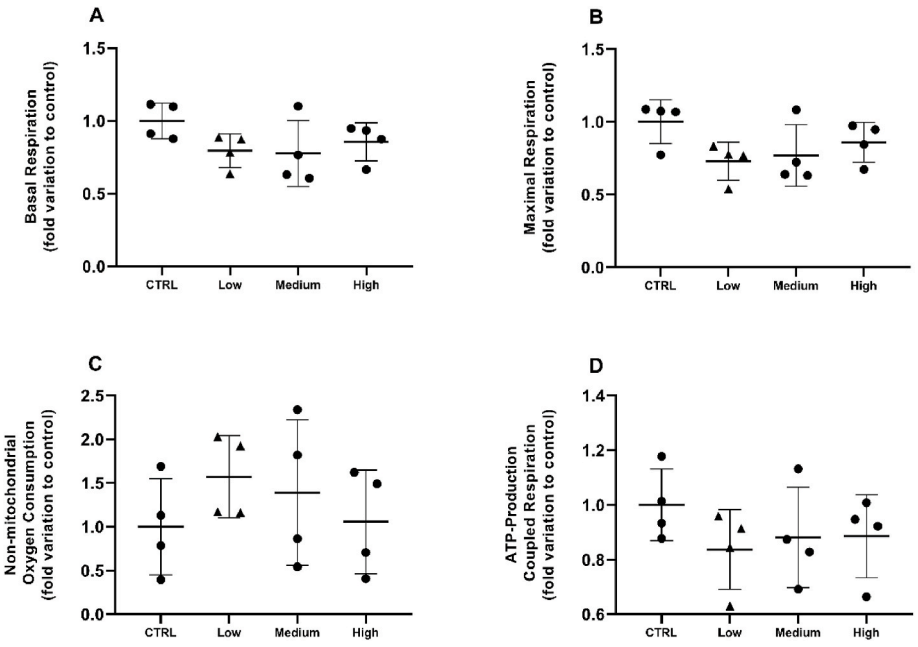

Fig. 3. Effects of sFlt-1/PlGF ratios on EC real-time mitochondrial basal respiration (A), maximal respiration (B), non-mitochondrial oxygen consumption (C), and ATP-production coupled respiration (D) assessed using a Seahorse XF Analyzer. ECs were untreated (CTRL) or treated for 24 h with low, medium, or high sFlt-1/PlGF ratios (1.6, 33.3, and 85.7, respectively). Data are expressed as mean ± SD (n = 4 for each condition) and also shown as fold-change relative to CTRL levels. ANOVA followed by Bonferroni's test. * ($p < 0.05$).

also remained unaffected by varying sFlt-1/PlGF ratios (Fig. 3D).

While proton leak, the movement of protons across the inner mitochondrial membrane independent of ATP synthase, showed no significant changes across the different sFlt-1/PlGF ratios (Fig. 4A), spare respiratory capacity (SRC), the reserve capacity of mitochondria to produce ATP under increased demand (Fig. 4B) was elevated in ECs exposed to the highest sFlt-1/PlGF ratio ($p < 0.05$). Finally, coupling efficiency, the percentage of respiration coupled to ATP synthesis, did not differ significantly between the groups (Fig. 4C). Fig. 4D shows the mitochondrial OCR over time after exposure to low, medium, high sFlt-1/PlGF ratios.

3.5. *sFlt-1/PlGF ratios drive distinct metabolic reprogramming in ECs*

We further investigated the metabolic impact of varying sFlt-1/PlGF ratios on ECs using a metabolomics analysis on supernatants collected from cells cultured for 24 h under low, medium, and high sFlt-1/PlGF ratios. Using PCA, we found a partial separation of groups, primarily along the first principal component (PC1), which explained 47.2 % of the variance while PC2 (y-axis) explained 17.6 %. Notably, the high sFlt-1/PlGF ratio appeared to cluster distinctly from the low and medium groups, suggesting potential metabolic differences between the ratios, and thus, an impact of sFlt-1/PlGF ratios on the metabolic profiles of ECs (Fig. 5A). PLS-DA further highlighted the separation between the ratios. The 3D plot demonstrated a clear distinction between the high sFlt-1/PlGF and the low/medium ratios, with minimal overlap of the 95 % confidence ellipsoids (Fig. 5B). To identify the metabolites driving the observed separation, we examined the VIP scores derived from the PLS-DA model. Several metabolites exhibited high VIP scores, indicating their significant contributions to distinguishing between the ratios. Notably, lactate, succinate, glucose, and glycine were the top-ranked metabolites (Fig. 5C). Box plots illustrated the relative concentrations of these metabolites across the different sFlt-1/PlGF ratios. Consistent with our PLS-DA results, we observed a significant increase in lactate and succinate levels after exposure to the high sFlt-1/PlGF ratio compared with exposure to the low and medium ratios. Glycine levels also showed a similar trend. In contrast, glucose levels significantly decreased after exposure to the high sFlt-1/PlGF ratio (Fig. 5D). Notably, the alterations in absolute concentrations of these metabolites followed a dose-dependent effect of sFlt-1/PlGF ratios.

4. Discussion

While the mechanisms through which angiogenic imbalance disrupts endothelial homeostasis and precedes the clinical manifestations of PE are well-established, they remain incompletely understood. Our study demonstrated a strong association between elevated circulating sFlt-1 levels in women with PE and specific metabolite levels, particularly succinate, glycine, and lactate. Furthermore, we provided a mechanistic explanation for these findings with an *in vitro* study, which showed that exposure of ECs to increasing sFlt-1/PlGF ratios induces metabolic alterations, oxidative stress, and mitochondrial dysfunction.

Our results revealed plasma lactate, succinate, and glycine levels positively correlated with elevated circulating sFlt-1 levels in women with PE, suggesting an endothelial metabolic dysfunction. Seahorse analysis demonstrated an increase in mitochondrial capacity in ECs exposed to high sFlt-1/PlGF ratios. This can be interpreted as an adaptive response to sustain ATP production under stress conditions. This increase was accompanied by elevated levels of 4-HNE, a marker of lipid peroxidation, which indicated that mitochondrial compensation was insufficient to prevent oxidative damage.

In addition to its role in the Krebs cycle, succinate may act as a signaling metabolite in response to hypoxia and inflammation. Under these conditions, succinate can accumulate in the cytoplasm, where it activates several signaling pathways, such as HIF-1 (hypoxia-inducible factor 1). Succinate may also activate receptors that lead to inflammation and angiogenesis [29,30]. Similarly, increased glycine levels in ECs and PE plasma may reflect impaired glutathione synthesis and reduced antioxidant defense. Glycine plays important roles in endothelial protection, redox balance, and placental function, and its dysregulation may contribute to fetal growth restriction [31–34]. It is important to highlight that while our findings demonstrate associations between circulating plasmatic sFlt-1 levels and some metabolites (mainly succinate and glycine), these changes may also reflect systemic metabolic

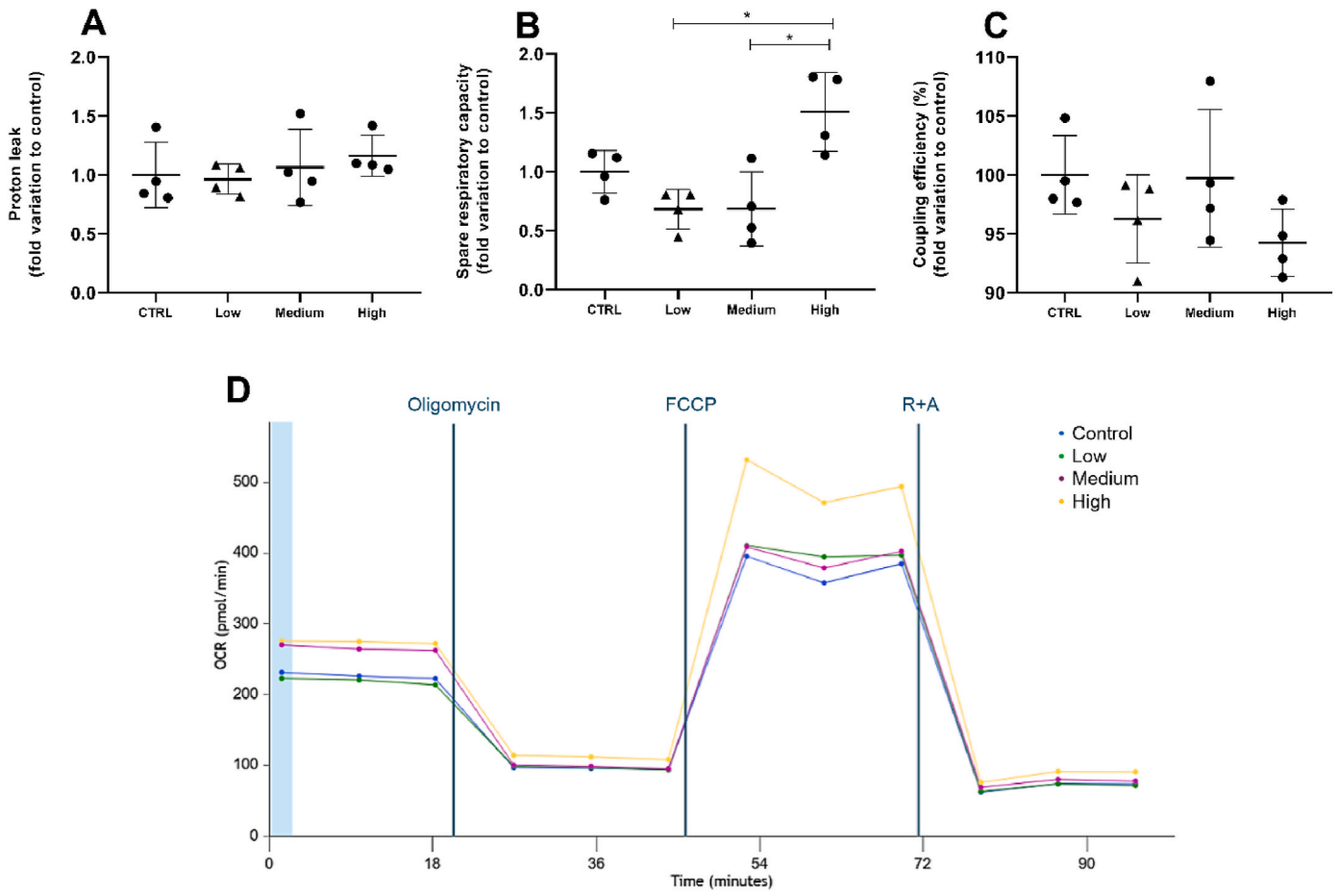

Fig. 4. Effects of sFlt-1/PlGF ratios on EC real-time proton leak (A), reserve capacity of mitochondria in absolute values (B), and the percentage of respiration coupled to ATP synthesis (C) using a Seahorse XF Analyzer. Mitochondrial oxygen consumption rate (OCR) profile in cells treated with increasing sFlt-1/PlGF ratios (D). Basal respiration was measured before the sequential addition of oligomycin (ATP synthase inhibitor), FCCP (uncoupler), and rotenone plus antimycin A (complex I and III inhibitors). ECs were untreated (CTRL) or treated for 24 h with low, medium, or high sFlt-1/PlGF ratios (1.6, 33.3, and 85.7, respectively). Data are expressed as mean ± SD (n = 4 for each condition) and also shown as fold variation relative to CTRL. ANOVA followed by Bonferroni's test. * ($p < 0.05$).

dysfunction in PE pathophysiology. Therefore, the metabolic alterations observed may serve as indices of disease severity or progression, independently of sFlt-1 effects. More longitudinal studies are needed to investigate the relationship among these variables.

The metabolism of glucose in ECs is an essential and complex process for maintaining vascular health, largely due to the role of these cells in regulating vascular tone, permeability, inflammation, and angiogenesis [35]. Elevated extracellular glucose levels enhance glucose uptake and stimulate its metabolism via glycolysis. ECs are reported to rapidly increase glucose metabolism via glycolysis in response to pro-angiogenic signals such as growth factors [36]. Some studies have described a relationship between hyperinsulinism during the oral glucose challenge test and the onset of gestational hypertension [37], while others showed that level of plasma glucose after a test positively correlated with the development of PE [38]. Evidence suggests that glucose metabolism might be connected to the angiogenic imbalance reported in PE, while another study discussed an altered angiogenic status and insulin resistance as a risk of developing PE and future cardiovascular diseases [39]. Our data showed no significant correlation between glucose and sFlt-1 levels in plasma of women with PE. However, we did observe a dose-dependent decrease in the glucose concentration of the culture medium with increasing sFlt-1/PlGF ratios in our *in vitro* studies. This finding may indicate that cells under these conditions exhibit significantly higher glucose uptake. This suggests a metabolic reprogramming towards glycolysis to sustain ATP production. However, lactate, the main end-product of glucose metabolism, can be exported from the cells, influencing both autocrine and paracrine signaling, and modulating vascular tone, cellular metabolism, and inflammatory pathways [40–43]. To support this assumption, we found that increasing sFlt-1/PlGF ratios induced a dose-dependent rise in lactate levels in ECs, which parallels the elevated circulating sFlt-1 levels observed in PE plasma. Increasing lactate levels often indicate hypoxia or activation of hypoxia-related pathways, which results in a decrease in the efficiency of pyruvate transport into the mitochondria [44], which is diverted to the cytoplasm, where it is converted into lactate by LDH. Despite pyruvate not appearing as an altered metabolite in our results, it appeared among the 13 most significant metabolites in VIP scores for group differentiation.

This study provides novel insights by considering clinical data alongside a mechanistic *in vitro* model using increasing sFlt-1/PlGF ratios. However, some limitations must be acknowledged. First, we measured only sFlt-1 in the plasma samples of women with PE, while our *in vitro* model evaluated the effects of the sFlt-1/PlGF ratio. The absence of PlGF quantification in patient samples limits direct translation of the *in vitro* findings. Future studies should assess both markers in maternal plasma to better correlate endothelial and metabolic responses. Furthermore, sFlt-1 levels were significantly higher in women who delivered preterm compared to those who delivered at term (data not shown), suggesting that gestational outcomes such as preterm birth, which represents a potential confounding factor, may also influence part of the metabolomics alterations. Investigation of stratified cohorts will be essential to delineate the respective contributions of angiogenic and

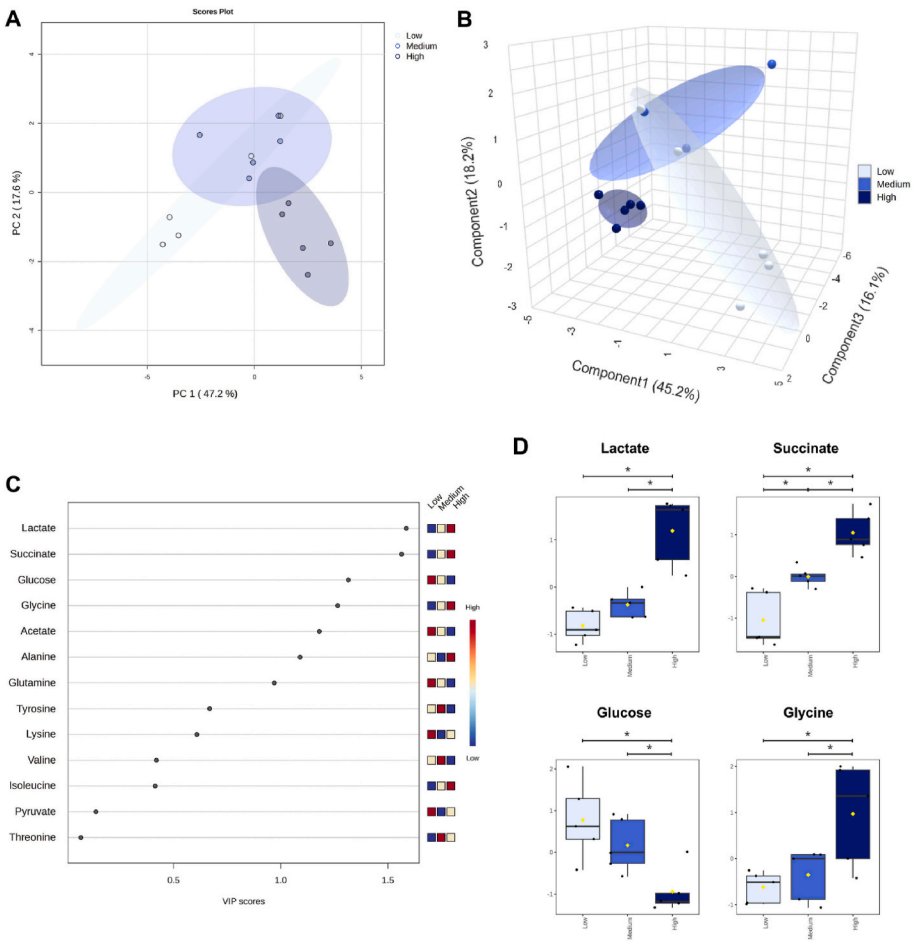

Fig. 5. Metabolomics profiling reveals distinct metabolics changes in ECs exposed to varying sFlt-1/PlGF ratios. Supernatants were collected from ECs cultured for 24 h with low (1.6), medium (33.3), and high (85.7) sFlt-1/PlGF ratios and subjected to metabolomics analysis. (A) A two-dimensional PCA score plot showing the overall metabolic differences. Each point represents one sample. (B) A 3D PLS-DA score plot revealing distinct separation, particularly between the high sFlt-1/PlGF ratio group and the others. (C) A VIP score plot identifying key metabolites contributing to group separation. Higher VIP scores (x-axis) indicate greater importance. Key metabolites include lactate, succinate, glucose, and glycine. (D) Box plots showing relative concentrations of these metabolites. Box plots represents n = 5 per group, *p < 0.05 (one-way ANOVA with Tukey post-hoc test).

metabolic alterations in PE and preterm births. Second, our cohort did not include a healthy normotensive pregnant control group, restricting interpretation of disease-specific changes. This, along with the relatively small number of biological replicates (n = 4–5) used in the *in vitro* experiments, may reduce the robustness and generalizability of the findings. Future studies with larger sample sizes and incorporating control groups are warranted to confirm these observations and to validate the specificity of these metabolite alterations. While we observed correlations between sFlt-1 and metabolite levels, these associations may reflect systemic metabolic dysfunction inherent to PE rather than direct causal effects of sFlt-1. Thus, longitudinal studies are needed to assess causality and the utility of these metabolites as biomarkers of disease progression. Finally, our study did not directly assess heme oxygenase-1 (HO-1) expression or activity. The observed oxidative stress and metabolic alterations associated with elevated sFlt-1/PlGF ratios may involve HO-1-mediated pathways, since it is a stress-inducible enzyme with well-established pleiotropic properties, including anti-inflammatory, antioxidant, and cytoprotective effects playing a critical role in regulating sFlt-1 levels and modulating endothelial function in the context of PE [45,46]. The induction of HO-1 has been shown to reduce sFlt-1 expression, thereby potentially ameliorating endothelial dysfunction and oxidative stress. Despite these limitations, our findings highlight a potential mechanistic link between an angiogenic imbalance and metabolic dysfunction in PE. Mitochondrial alterations, oxidative stress, and changes in key metabolites such as glycine and succinate may underlie disease severity and progression. Targeting these pathways may provide new avenues for therapeutic intervention aimed at improving endothelial and placental function. Moreover, the identification of metabolite signatures associated with sFlt-1 levels could contribute to risk stratification and earlier diagnosis of PE or strategies to enhance mitochondrial function, potentially ameliorating PE severity.

CRediT authorship contribution statement

Priscila R. Nunes: Writing – review & editing, Writing – original draft, Validation, Methodology, Investigation, Formal analysis, Data curation. **Ricardo M. Bruder:** Writing – review & editing, Methodology, Investigation, Formal analysis, Data curation. **Julyane N.S. Kaihara:** Writing – review & editing, Methodology, Investigation, Formal analysis. **Fabio R. de Moraes:** Writing – review & editing, Methodology, Investigation, Formal analysis. **Ljubica Tasic:** Writing – review & editing, Methodology, Formal analysis, Data curation. **Raquel L. Bernardino:** Writing – review & editing, Validation, Investigation. **Patricia Braga:** Writing – review & editing, Methodology, Formal analysis. **Pedro F. Oliveira:** Writing – review & editing, Writing – original draft, Supervision, Project administration, Investigation, Funding acquisition. **Irene Rebelo:** Writing – review & editing, Validation, Supervision, Investigation, Funding acquisition. **Margarida Fardilha:** Writing –

review & editing, Supervision. **Ricardo C. Cavalli:** Writing – review & editing, Supervision, Formal analysis. **Valeria C. Sandrim:** Writing – review & editing, Supervision, Project administration, Funding acquisition, Formal analysis, Data curation. **Marco G. Alves:** Writing – review & editing, Writing – original draft, Supervision, Project administration, Methodology, Investigation, Funding acquisition, Formal analysis, Conceptualization.

Funding

This research was funded by Fundacao de Amparo a Pesquisa do Estado de São Paulo (FAPESP), grant numbers: 2018/24069–3 (LT); 2021/12010–7 (VCS); 2022/07226–3 (PRN); and 2023/08897–1 (JNSK). This work was also funded by Conselho Nacional de Desenvolvimento Científico e Tecnológico (CNPq), grant numbers 308504/2021–6 (VCS); 308079/2021–3 (LT); 301419/2022–1 (RCC); and Coordenação de Aperfeiçoamento de Pessoal de Nível Superior (CAPES) grant number 88887.826908/2023–00 (RMB). This research was also funded by "Fundação para a Ciência e a Tecnologia"—FCT to UMIB (UIDB/00215/2020 - DOI 10.54499/UIDB/00215/2020, and UIDP/00215/2020 - DOI 10.54499/UIDP/00215/2020), ITR—Laboratory for Integrative and Translational Research in Population Health (LA/P/0064/2020 - DOI 10.54499/LA/P/0064/2020). The work was co-funded by FEDER through the COMPETE/QREN, FSE/POPH and POCI—COMPETE 2020 (POCI-01-0145-FEDER-007491) funds. PFO is funded by national funds through FCT—Fundação para a Ciência e a Tecnologia, I.P., under the Scientific Employment Stimulus-Institutional Call-reference CEEC-INST/00026/2018. This work also received support and help from FCT/MCTES to LAQV-REQUIMTE (LA/P/0008/202 - DOI 10.54499/LA/P/0008/2020; UIDP/50006/2020 - DOI 10.54499/UIDP/50006/2020; and UIDB/50006/2020 - DOI 10.54499/UIDB/50006/2020) and to iBiMed (UIDB/04501/2020 - DOI 10.54499/UIDB/04501/2020 and UIDP/04501/2020 - DOI 10.54499/UIDP/04501/2020), through national funds. The 500 MHz Bruker Avance III HD spectrometer is part of the National Portuguese NMR Network (PTNMR), partially supported by Infrastructure Project No. 022161 (cofinanced by FEDER through COMPETE 2020, POCI, and PORL and FCT through PIDDAC).

Declaration of competing interest

The authors declare the following financial interests/personal relationships which may be considered as potential competing interests: Ricardo Miguel Bruder reports financial support was provided by Coordination of Higher Education Personnel Improvement. Valeria Cristina Sandrim reports financial support was provided by National Council for Scientific and Technological Research. Ljubica Tasic reports financial support was provided by National Council for Scientific and Technological Development. Ricardo de Carvalho Cavalli reports financial support was provided by National Council for Scientific and Technological Development. Valeria Cristina Sandrim reports financial support was provided by State of Sao Paulo Research Foundation. Ljubica Tasic reports financial support was provided by State of Sao Paulo Research Foundation. Priscila Rezeck Nunes reports financial support was provided by State of Sao Paulo Research Foundation. Julyane Natsumi Saito Kaihara reports financial support was provided by State of Sao Paulo Research Foundation. This research was also funded by "Fundação para a Ciência e a Tecnologia"—FCT to UMIB (UIDB/00215/2020 - DOI 10.54499/UIDB/00215/2020, and UIDP/00215/2020 - DOI 10.54499/UIDP/00215/2020), ITR—Laboratory for Integrative and Translational Research in Population Health (LA/P/0064/2020 - DOI 10.54499/LA/P/0064/2020). The work was co-funded by FEDER through the COMPETE/QREN, FSE/POPH and POCI—COMPETE 2020 (POCI-01-0145-FEDER-007491) funds. Pedro F. Oliveira is funded by national funds through FCT—Fundação para a Ciência e a Tecnologia, I.P., under the Scientific Employment Stimulus-Institutional Call-reference CEEC-INST/00026/2018. This work also received support and help from FCT/MCTES to LAQV-REQUIMTE (LA/P/0008/202 - DOI 10.54499/LA/P/0008/2020; UIDP/50006/2020 - DOI 10.54499/UIDP/50006/2020; and UIDB/50006/2020 - DOI 10.54499/UIDB/50006/2020) and to iBiMed (UIDB/04501/2020 - DOI 10.54499/UIDB/04501/2020 and UIDP/04501/2020 - DOI 10.54499/UIDP/04501/2020), through national funds. If there are other authors, they declare that they have no known competing financial interests or personal relationships that could have appeared to influence the work reported in this paper.

Appendix A. Supplementary data

Supplementary data to this article can be found online at https://doi.org/10.1016/j.placenta.2025.09.018.

References

[1] American College of Obstetricians and Gynecologists, Gestational hypertension and preeclampsia: ACOG practice bulletin, No. 222, Obstet. Gynecol. 135 (6) (2020) e237–e260.
[2] S. Rana, S.D. Burke, S.A. Karumanchi, Imbalances in circulating angiogenic factors in the pathophysiology of preeclampsia and related disorders, Am. J. Obstet. Gynecol. 226 (2S) (2022) S1019–S1034.
[3] J. Gao, J. Shen, Y. Jiang, et al., Value of second trimester maternal serum sFlt-1, PlGF and their ratio in the prediction of preeclampsia, Zhonghua Fu Chan Ke Za Zhi 49 (1) (2014) 22–25.
[4] X. Bian, A. Biswas, X. Huang, et al., Short-term prediction of adverse outcomes using the sFlt-1 (soluble fms-like tyrosine kinase 1)/PlGF (placental growth factor) ratio in Asian women with suspected preeclampsia, Hypertension 74 (1) (2019) 164–172.
[5] U. Sovio, F. Gaccioli, E. Cook, et al., Prediction of preeclampsia using the soluble fms-like tyrosine kinase 1 to placental growth factor ratio: a prospective cohort study of unselected nulliparous women, Hypertension 69 (4) (2017) 731–738.
[6] R. Thadhani, A.S. Cerdeira, S.A. Karumanchi, Translation of mechanistic advances in preeclampsia to the clinic: Long and winding road, FASEB J. 38 (1) (2024) e23441.
[7] C.E. Powe, R.J. Levine, S.A. Karumanchi, Preeclampsia, a disease of the maternal endothelium: the role of antiangiogenic factors and implications for later cardiovascular disease, Circulation 123 (24) (2011) 2856–2869.
[8] R.J. Levine, S.E. Maynard, C. Qian, et al., Circulating angiogenic factors and the risk of preeclampsia, N. Engl. J. Med. 350 (7) (2004) 672–683.
[9] S. Verlohren, S.P. Brennecke, A. Galindo, et al., Clinical interpretation and implementation of the sFlt-1/PlGF ratio in the prediction, diagnosis and management of preeclampsia, Pregnancy Hypertens 27 (2022) 42–50.
[10] M. Hund, D. Allegranza, M. Schoedl, et al., Multicenter prospective clinical study to evaluate the prediction of short-term outcome in pregnant women with suspected preeclampsia (PROGNOSIS): study protocol, BMC Pregnancy Childbirth 14 (2014) 324.
[11] H. Zeisler, E. Llurba, F. Chantraine, et al., Predictive value of the sFlt-1:PlGF ratio in women with suspected preeclampsia, N. Engl. J. Med. 374 (1) (2016) 13–22.
[12] I. Herraiz, E. Simón, P.I. Gómez-Arriaga, et al., Clinical implementation of the sFlt-1/PlGF ratio to identify preeclampsia and fetal growth restriction: a prospective cohort study, Pregnancy Hypertens 13 (2018) 279–285.
[13] L.A. Dröge, F.H. Perschel, N. Stütz, et al., Prediction of preeclampsia-related adverse outcomes with the sFlt-1/PlGF ratio in the clinical routine: a real-world study, Hypertension 77 (2) (2021) 461–471.
[14] H. Li, B. Gu, Y. Zhang, et al., Hypoxia-induced increase in soluble Flt-1 production correlates with enhanced oxidative stress in trophoblast cells from the human placenta, Placenta 26 (2–3) (2005) 210–217.
[15] E.O. Anto, D.A. Coall, O. Addai-Mensah, et al., Early gestational profiling of oxidative stress and angiogenic growth mediators as predictive, preventive and personalised (3P) medical approach to identify suboptimal health pregnant mothers likely to develop preeclampsia, EPMA J. 12 (4) (2021) 517–534.
[16] K.R. Castro, K.M. Prado, A.R. Lorenzon, et al., Serum from preeclamptic women triggers endoplasmic reticulum stress pathway and expression of angiogenic factors in trophoblast cells, Front. Physiol. 12 (2022) 799653.
[17] D.S. Charnock-Jones, Placental hypoxia, endoplasmic reticulum stress and maternal endothelial sensitisation by sFLT1 in pre-eclampsia, J. Reprod. Immunol. 114 (2016) 81–85.
[18] S. Shinohara, N. Hiraoka, K. Mochizuki, et al., sFlt-1/PlGF ratio predicts serious outcomes in confirmed early-onset preeclampsia, Eur. J. Obstet. Gynecol. Reprod. Biol. 300 (2024) 159–163.
[19] J. Espinoza, A. Vidaeff, C.M. Pettker, H. Simhan, Gestational hypertension and preeclampsia, Obstet. Gynecol. 133 (1) (2019) e1–e25.
[20] P. Nikuei, M. Rajaei, K. Malekzadeh, et al., Accuracy of soluble endoglin for diagnosis of preeclampsia and its severity, Iran. Biomed. J. 21 (5) (2017) 312–320.
[21] D. Tannetta, I. Masliukaite, M. Vatish, et al., Update of syncytiotrophoblast derived extracellular vesicles in normal pregnancy and preeclampsia, J. Reprod. Immunol. 119 (2017) 98–106.

[22] C.W. Redman, I.L. Sargent, A.C. Staff, IFPA Senior Award Lecture: making sense of pre-eclampsia – two placental causes of preeclampsia? Placenta 35 (Suppl) (2014) S20–S25.
[23] X.Q. Hu, L. Zhang, Mitochondrial dysfunction in the pathogenesis of preeclampsia, Curr. Hypertens. Rep. 24 (3) (2022) 157–172.
[24] P.R. Nunes, P.F. Oliveira, I. Rebelo, et al., Relevance of real-time analyzers to determine mitochondrial quality in endothelial cells and oxidative stress in preeclampsia, Vasc. Pharmacol. (2024) 107372.
[25] T.M. Michelsen, A.M. Holme, M.B. Holm, et al., Uteroplacental glucose uptake and fetal glucose consumption: a quantitative study in human pregnancies, J. Clin. Endocrinol. Metab. 104 (3) (2019) 873–882.
[26] N.S. Karpova, O.P. Dmitrenko, T.S. Budykina, Literature review: the sFlt1/PlGF ratio and pregestational maternal comorbidities: new risk factors to predict pre-eclampsia, Int. J. Mol. Sci. 24 (12) (2023) 6744.
[27] P.R. Nunes, T.O. Bueno Pereira, Matheus M. Bertozzi, et al., Glibenclamide increases nitric oxide levels and decreases oxidative stress in an in vitro model of preeclampsia, Antioxidants 11 (9) (2022) 1620.
[28] D.S. Wishart, A. Guo, E. Oler, et al., Hmdb 5.0: the human metabolome database for 2022, Nucleic Acids Res. 50 (D1) (2022) D622–D631.
[29] G.M. Tannahill, A.M. Curtis, J. Adamik, et al., Succinate is an inflammatory signal that induces IL-1β through HIF-1α, Nature 496 (7444) (2013) 238–242.
[30] M.A. Selak, S.M. Armour, E.D. MacKenzie, et al., Succinate links TCA cycle dysfunction to oncogenesis by inhibiting HIF-α prolyl hydroxylase, Cancer Cell 7 (1) (2005) 77–85.
[31] T.R.H. Regnault, J.E. Friedman, R.B. Wilkening, et al., Fetoplacental transport and utilization of amino acids in IUGR – a review, Placenta 26 (Suppl A) (2005) S52–S62.
[32] G. Liu, W. Deng, W. Cui, et al., Analysis of amino acid and acyl carnitine profiles in maternal and fetal serum from preeclampsia patients, J. Matern. Fetal Neonatal Med. 33 (16) (2020) 2743–2750.
[33] N. Prameswari, R. Irwinda, N. Wibowo, Y.B. Saroyo, Maternal amino acid status in severe preeclampsia: a cross-sectional study, Nutrients 14 (5) (2022) 1019.
[34] S.C. Lu, Glutathione synthesis, Biochim. Biophys. Acta 1830 (5) (2013) 3143–3153.
[35] A.M. Clyne, Endothelial response to glucose: dysfunction, metabolism, and transport, Biochem. Soc. Trans. 49 (1) (2021) 313–325.
[36] P. Yu, K. Wilhelm, A. Dubrac, et al., FGF-dependent metabolic control of vascular development, Nature 545 (7653) (2017) 224–228.
[37] H. Valensise, G. Larciprete, B. Vasapollo, et al., C-peptide and insulin levels at 24–30 weeks' gestation: an increased risk of adverse pregnancy outcomes? Eur. J. Obstet. Gynecol. Reprod. Biol. 103 (2) (2002) 130–135.
[38] G.M. Joffe, J.R. Esterlitz, R.J. Levine, et al., The relationship between abnormal glucose tolerance and hypertensive disorders of pregnancy in healthy nulliparous women, Am. J. Obstet. Gynecol. 179 (4) (1998) 1032–1037.
[39] M. Wolf, C.A. Hubel, C. Lam, et al., Preeclampsia and future cardiovascular disease: potential role of altered angiogenesis and insulin resistance, J. Clin. Endocrinol. Metab. 89 (12) (2004) 6239–6243.
[40] R. Hoque, A. Farooq, A. Ghani, et al., Lactate reduces liver and pancreatic injury in toll-like receptor– and inflammasome-mediated inflammation via GPR81-mediated suppression of innate immunity, Gastroenterology 146 (7) (2014) 1763–1774.
[41] K. De Bock, M. Georgiadou, S. Schoors, et al., Role of PFKFB3-driven glycolysis in vessel sprouting, Cell 154 (3) (2013) 651–663.
[42] G.A. Brooks, Cell–cell and intracellular lactate shuttles, J Physiol. 587 (Pt 23) (2009) 5591–5600.
[43] P. Sonveaux, F. Végran, T. Schroeder, et al., Targeting lactate-fueled respiration selectively kills hypoxic tumor cells in mice, J. Clin. Investig. 118 (12) (2008) 3930–3942.
[44] D. Wang, Q. Wang, G. Yan, et al., Hypoxia induces lactate secretion and glycolytic efflux by downregulating mitochondrial pyruvate carrier levels in human umbilical vein endothelial cells, Mol. Med. Rep. 18 (2) (2018) 1710–1717.
[45] E.M. George, J.P. Granger, Heme oxygenase in pregnancy and preeclampsia, Curr. Opin. Nephrol. Hypertens. 22 (2) (2013) 156–162.
[46] M. Cudmore, S. Ahmad, B. Al-Ani, et al., Negative regulation of soluble Flt-1 and soluble endoglin release by heme oxygenase-1, Circulation 115 (13) (2007) 1789–1797.